Microkinetic Study of CO Oxidation and PROX on Ir−Fe Catalyst

Kuo Liu,[†,‡] Aiqin Wang,[†] Wansheng Zhang,[†] Junhu Wang,[†] Yanqiang Huang,[†] Xiaodong Wang,[†] Jianyi Shen,*[,§] and Tao Zhang*[,†]

State Key Laboratory of Catalysis, Dalian Institute of Chemical Physics, Chinese Academy of Sciences, 457 Zhongshan Road, Dalian 116023, P. R. China, Graduate University of Chinese Academy of Sciences, Beijing 100049, P. R. China, and Department of Chemistry, Nanjing University, Nanjing 210093, P. R. China

A microkinetic analysis of the preferential oxidation of CO in H_2 over Ir−Fe/SiO_2 catalyst is reported. Based on the results of in situ diffuse reflectance infrared spectroscopy, microcalorimetry, Mössbauer spectroscopy, and steady-state kinetic experiments in a microreactor, a microkinetic model is proposed that predicts the experimental results well. The model suggests that the reaction between adsorbed H and O for the formation of OH is rate-limiting for the PROX reaction, whereas the surface reaction between adsorbed CO and O is rate-determining for CO oxidation. In addition, the model predicts that the oxidation of adsorbed CO by surface OH is the dominant pathway for the PROX reaction. The surface coverages of different intermediates are also predicted by the model. According to this model, we can conclude that the presence of H_2 increases the surface concentration of OH and, hence, lowers the activation energy and increases the rate of the PROX reaction.

1. Introduction

The preferential oxidation of CO (PROX) has been considered as a promising approach for the removal of low concentrations of CO from H_2 gas to provide clean, CO-free hydrogen fuel for proton-exchange membrane fuel cells (PEMFCs). So far, among a vast number of catalyst formulations, noble metals (Au, Pt, Ir, etc.) supported on or promoted with a reducible oxide (TiO_2, Fe_2O_3, CeO_2, etc.) have been established as a class of very active catalysts, especially at low temperatures.[1–4] For this type of catalyst, a dual-site adsorption mechanism has been proposed, where CO adsorbed on noble-metal sites reacts with oxygen activated on reducible oxide at the metal/oxide interface.[5,6] In this mechanism, however, H_2 is not involved. Actually, the H_2 in the reaction mixture has a significant impact on CO oxidation, in terms of both activity and selectivity. As shown in the equations

$$CO + {}^1/_2O_2 \rightarrow CO_2 \qquad \Delta H^\circ_{298} = -283 \text{ kJ/mol}$$

and

$$H_2 + {}^1/_2O_2 \rightarrow H_2O \qquad \Delta H^\circ_{298} = -242 \text{ kJ/mol}$$

the oxidation of H_2 takes place in competition with CO oxidation, which becomes more pronounced at high temperatures and leads to a dramatic decrease in the selectivity of CO oxidation.[7] On the other hand, various studies have shown that H_2 promotes low-temperature CO oxidation, although the promotion mechanism is under debate.[8–10]

Previously, we reported that Ir−Fe/SiO_2 catalyst is highly active and selective for the PROX reaction.[11] Compared with Ir/SiO_2, the addition of Fe not only weakens the adsorption of CO or H_2 on the Ir sites, but also greatly increases the adsorption of O_2 on the FeO_x sites. The H_2 in the reaction stream, even in a very low amount, can significantly increase the low-temperature CO conversions. Moreover, the promotional effect of H_2 on the CO oxidation rate is marked on the Ir−Fe/SiO_2 catalyst compared with the Ir/SiO_2 catalyst. By means of quasi in situ Mössbauer spectroscopy,[12] we found that the H_2 concentration in the reaction stream affects the amount of Fe^{2+}, which was identified as the active site for oxygen adsorption. Nevertheless, we observed a slight discrepancy between the activity and the Fe^{2+} content at the point of 2% H_2, which suggests that the amount of Fe^{2+} on the catalyst surface might not be the only factor determining the high activity of Ir−Fe catalyst. Instead, H_2 might directly participate in the reaction by forming surface OH, which was reported to react with adsorbed CO to form carboxylate that then decomposes to give CO_2.[13] To gain a better understanding of the effect of H_2 on CO oxidation, herein, we report a microkinetic study of the PROX reaction on Ir−Fe catalyst with and without the presence of H_2 in the reaction stream.

For noble-metal catalysts, several different kinetic rate expressions have been reported. Literature values of the power constants of CO oxidation range from 0.7 to 1.0 for oxygen and from −1.5 to 0 for CO, with the apparent activation energy for CO oxidation between 55 and 80 kJ/mol over Pt catalysts.[14–17] Both CO oxidation and H_2 oxidation are limited by the presence of a CO adlayer.[18] Nevertheless, kinetic studies on Pt-based catalysts combined with reducible metal oxides in the PROX reaction are comparatively fewer. Choi and Stenger[19] proposed a kinetic model for CO oxidation on Pt−Fe catalyst based on three reactions (CO oxidation, H_2 oxidation, and the water−gas shift reaction). Unlike for the mechanism on the single-metal catalyst, the rate-determining step was not CO desorption on bimetallic catalyst, as suggested by Schubert et al.[20]

However, there are limits to the information that can be determined from experimental data by global kinetics. For example, it is difficult to discriminate between different reaction mechanisms because different kinetic expressions might fit the experimental data equally well. Therefore, it is impossible to determine the mechanism from an empirical kinetic expression. Consequently, the development of microkinetic models based

* To whom correspondence should be addressed. Tel.: +86-411-84379015 (T.Z.). Fax: +86-411-84685940 (T.Z.). E-mail: taozhang@dicp.ac.cn (T.Z.), jyshen@nju.edu.cn (J.S.).

† State Key Laboratory of Catalysis, Dalian Institute of Chemical Physics, Chinese Academy of Sciences.

‡ Graduate University of Chinese Academy of Sciences.

§ Nanjing University.

10.1021/ie1009052
Published on Web 12/01/2010

Table 1. Bond Strengths (Q), Bond Dissociation Energies in the Gas Phase (D), Adsorption Enthalpies (ΔH), and Uptakes (N) of Different Species in the PROX Reaction on Ir−Fe Catalyst

	D (kJ/mol)	Q (kJ/mol)	ΔH (kJ/mol)[a]	N (μmol/g_{cat})[a]
CO	1076	112	70	20
O_2	498		400	240
H_2	436		25	
CO_2	1606	7		
H		230		
O		449		
OH	427	232		
H_2O	926	47		

[a] Measured by microcalorimetry at 313 K.

on knowledge of elementary steps and energetics has attracted much attention.[21–27] The advantage of developing microkinetic models is that it is not necessary to make simplifications to reduce the rate expression to a closed analytical form. The microkinetic approach attempts to describe reactions using their most fundamental set of elementary reaction steps, without assuming a rate-determining step (RDS), a most abundant surface species, or some other simplification that would limit the range of applicability of the model. The mapping between microkinetics and global kinetics is unidirectional, as global kinetics can be obtained from microkinetics but the opposite is generally not the case. Recently, extensive work has been devoted to the catalytic oxidation of H_2 and CO on transition metals, and a number of microkinetic models have been proposed, especially for single-metal catalysts.[28–30] Mhadeshwar and Vlachos[31] suggested a model on Pt that is capable of describing CO oxidation, H_2 oxidation, water−gas shift, and PROX reaction, by including CO−H_2 coupling through the CO + OH reaction, as well as an indirect pathway through the carboxyl intermediate. Redox mechanisms involving CO reacting with oxidant O, obtained either by direct adsorption of O_2[32] or by a species generated by single H abstraction from water,[33] have been proposed. In comparison with these studies on single-metal catalysts, microkinetic studies of the PROX reaction on bimetallic catalysts are still seriously lacking.

2. Experimental Section

2.1. Catalyst Preparation and Characterization. The preparation and characterization of the Ir−Fe/SiO_2 catalyst was reported previously.[12] In short, Ir−Fe/SiO_2 was prepared by impregnation of SiO_2 (S_{BET} = 400 m^2/g) with an aqueous mixture of chloroiridic acid and ferric nitrate, followed by drying at 353 K for more than 8 h and calcination at 573 K for 5 h in air. The Ir content was fixed at 3 wt %, with an Fe/Ir atomic ratio of 5/1. The differential heats of adsorption were measured using a BT2.15 heat-flux microcalorimeter, and those values used in this work are summarized in Table 1.

In situ diffuse reflectance infrared spectroscopy (DRIFTS) was performed with a Bruker Equinox 55 spectrometer, equipped with a mercury cadmium telluride (MCT) detector and operated at a resolution of 4 cm^{-1}. Before each experiment, a sample of 15 mg in powder form was reduced in situ with H_2 at 573 K for 1 h. After the sample had been cooled to 373 K, PROX mixture gas (40% H_2, 2% CO, 1% O_2 in He) or CO oxidation gas (2% CO, 1% O_2 in He) was introduced into the reaction cell at a total flow rate of 100 mL/min. The spectra were recorded against a background of the sample at 373 K under flowing He. All spectra were obtained under steady-state conditions.

2.2. Collection of Kinetic Data for the Reactions. The catalytic activities were evaluated in a fixed-bed reactor with a 10-mm inner diameter at atmospheric pressure. Before the test, the catalyst was reduced in situ with hydrogen at 573 K for 2 h. Then, ~20 mg of Ir−Fe/SiO_2 catalyst diluted with 100−150 mg of SiC was loaded into a reactor with a catalyst bed length of 2 mm. To eliminate the effects of diffusion, a total gas flow rate of 50 mL/min was used, which corresponds to a space velocity of 150 000−600 000 mL/(h g_{Cat}). Under differential conditions, the CO conversion was less than 20% in the temperature range of 323−403 K. The feed gas mixture is composed of 2 vol % CO, 1 vol % O_2, x vol % H_2 (x = 0−40), and the balance He. The effluent gas was analyzed using an online gas chromatograph system (Agilent GC-6890) equipped with a thermal conductivity detector. CO_2 and H_2O were detected as the only products. No methane was found under our experimental conditions. The reaction rates for the formation of CO_2 [mol/(s g_{Cat})] were calculated according to the flow rates, the conversion of CO, and the selectivity to CO_2. Then, the turnover frequencies (TOFs) were derived by considering the surface iridium sites titrated by CO adsorption at 313 K. The rates were calculated as follows:

CO conversion (X_{CO}) was calculated as

$$X_{CO}\,(\%) = \frac{[CO]_{in} - [CO]_{out}}{[CO]_{in}} \times 100$$

CO oxidation rates (s^{-1}) were calculated as

$$r_{CO} = \frac{X_{CO} Y_{CO,in} V_{gas}}{m_{cat} n_{cat}}$$

where m_{cat} is the mass of the catalyst in the catalytic bed in grams, n_{cat} is the number of the active site (Ir sites for our catalyst) in moles per gram of catalyst, V_{gas} is the total molar flow rate in moles per second, X_{CO} is the conversion of CO, and $Y_{CO,in}$ is the molar fraction of CO in the inlet gas mixture.

3. Method of Calculation of Microkinetic Parameters

The rate constants were estimated according to transition state theory, where the critical assumption is the quasi-equilibrium established between the reactants and an activated complex, as described in detail by Dumesic et al.[27]

Initial heats of adsorption were measured and taken as the estimation of activation energies for desorption steps: $E_d - E_a = -\Delta H_{ads}$, where ΔH_{ads} is the adsorption enthalpy measured calorimetrically. In the case of CO adsorption, because there is a steep decrease in adsorption energy from the initial value (120 kJ/mol),[12] we used the average value (70 kJ/mol) as the activation energy for CO desorption. For the surface reaction steps, where the enthalpy (ΔH) cannot be measured calorimetrically, the unity bond index-quadratic exponential potential (UBI-QEP) method described by Shustorovich and Sellers[34] was applied. The theoretical analysis is based on calculations of the heats of bond strength (Q), enthalpy changes (ΔH), and activation barriers (E) for most of the forward and reverse elementary reactions.[35] The bond strength between Ir and C for the adsorption of CO (Q_{Ir-CO}) can be calculated according to the equation

$$\Delta H_{CO} = Q_{Ir-CO}{}^{2}(Q_{Ir-CO} + D_{CO})^{-1}$$

and those for the adsorption of O_2 and H_2 can be calculated by the equation

$$Q_{0A} = 2^{-1}(D_{A2} - \Delta H_{A2})$$

where Q_{0A} is the bond strength of either the Fe−O or Ir−H bond (i.e., Q_{Fe-O} or Q_{Ir-H}, respectively).[27] The bond strengths of weakly adsorbed molecules, such as CO_2 and H_2O, were calculated using the equation

$$Q_{AB} = Q_{0A}^{2}(Q_{0A} + D_{AB})^{-1}$$

where D_{AB} is the dissociation energy for breaking a bond in CO_2 or H_2O in the gas phase and Q_{AB} is the bond strength between Ir and C for the adsorption of CO_2 (Q_{Ir-CO_2}) or between Fe and O for the adsorption of H_2O (Q_{Fe-OH_2}). Strong bonding for molecular radicals with unpaired electrons, such as OH, is calculated as

$$Q_{AB} = Q_{0A}^{2}(Q_{0A} + D_{AB})^{-1}$$

where D_{AB} is the dissociation energy of gas-phase OH, Q_{0A} is Q_{Fe-O}, and Q_{AB} is the bond strength of OH on the surface of Fe. For reactions such as AB → A + B, the activation energies for the forward reactions were calculated by

$$E_f = 2^{-1}[\Delta H + Q_A Q_B (Q_A + Q_B)^{-1}]$$

where $\Delta H = D + Q_{AB} - Q_A - Q_B$ and $D = D_{AB} - D_A - D_B = D_{AB}$. For disproportionation reactions such as A + BC → AB + C

$$E_f = 2^{-1}[\Delta H + Q_{AB} Q_C (Q_{AB} + Q_C)^{-1}]$$

where $\Delta H = D + Q_A + Q_{BC} - Q_{AB} - Q_C$ and $D = D_A + D_{BC} - D_{AB} - D_C$. D is the difference of dissociation energies between reactants and products. The activation energies (E_r) for the reverse reactions can be calculated in a similar way or by the relation equation $E_r = E_f - \Delta H$. Adsorbate−adsorbate interactions were not taken into consideration in this study. The calculated values of D, Q, and ΔH are listed in Table 1.

The number of active sites is important in determining the activity. As reported in our earlier studies,[11,36] CO and H_2 are activated on Ir sites, whereas O_2 is activated on Fe sites for the PROX reaction on Ir−Fe catalysts. After the reduction, the uptake of CO on the Ir−Fe/SiO_2 catalyst was measured to be 20 μmol/g_{cat}, which is assumed to be the number of active sites on Ir for the reaction, although all of the absorption sites are not necessarily all active. On the other hand, determination of the active sites on Fe is somewhat complex. The total amount of iron (N_{Fe}) in the Ir−Fe catalyst was about 800 μmol/g_{cat}. A Mössbauer study revealed that Fe^{2+} was the active site for the activation of O_2 and that the H_2 concentration in the feed stream influenced greatly the amount of Fe^{2+}.[12] For the steady-state PROX reaction at 353 K, it was found that the percentages of Fe^{2+} in the Ir−Fe catalyst were 4%, 14%, 17%, and 18% at H_2 concentration of 0%, 2%, 10%, and 40%, respectively. Thereby, the corresponding concentrations of active Fe^{2+} sites in the Ir−Fe catalyst were calculated to be 30, 110, 136, and 144 μmol/g_{cat}. Assuming that an oxygen atom adsorbs on two Fe^{2+} sites,[37] the number of active sites of Fe^{2+} can be roughly estimated to be 15, 56, 68, and 72 μmol/g_{cat} for the H_2 concentration of 0, 2, 10 and 40%, respectively. Thus, the ratio of active sites of Ir to Fe^{2+} in the Ir−Fe catalyst was determined as 20/15 for the absence of H_2 (CO oxidation only) and 20/55, 20/68, and 20/72 for the presence of 2%, 10%, and 40% H_2 (PROX reaction), respectively.

4. Microkinetic Models and Analysis

4.1. Reaction Model. The elementary steps involved in the PROX reaction[28,38] on the Ir−Fe catalyst can be described as

$$CO + Ir \rightleftarrows Ir - CO \quad (1)$$

$$O_2 + 2* \rightarrow 2O* \quad (2)$$

$$Ir - CO + O^{-}* \rightarrow CO_2 + Ir + * \quad (3)$$

$$H_2 + 2Ir \rightleftarrows 2H - Ir \quad (4)$$

$$H - Ir + O^{-}* \rightleftarrows OH^{-}* + Ir \quad (5)$$

$$OH^{-}* + H - Ir \rightarrow H_2O + *{+}Ir \quad (6)$$

$$OH^{-}* + Ir - CO \rightarrow CO_2 + H - Ir + * \quad (7)$$

where * denotes a reduced iron site (Fe^{2+}). In the absence of H_2 (i.e., CO oxidation only), only steps 1−3 are involved in the reaction model.[30,39] The first step involves the adsorption of CO, whose initial heat was measured to be 120 kJ/mol. Because the adsorption energy decreases rapidly with the CO coverage,[12] we used an average value of 70 kJ/mol as an estimation of the activation energy for the desorption of CO. The second step involves the adsorption of O_2 on the Fe^{2+} sites. The large adsorption heat of O_2 on the Ir−Fe catalyst (400 kJ/mol) does not allow the desorption of oxygen at the reaction temperatures, so step 2 can be considered irreversible. The reverse reaction of step 3 can be taken as the dissociative adsorption of CO_2 on the Ir−Fe catalyst. Because no adsorption of CO_2 was observed microcalorimetrically on the reduced Ir−Fe catalyst, step 3 (i.e., the reaction of adsorbed CO and O for the formation of CO_2) can be considered irreversible.

Based on the ratio of active sites of Ir to Fe^{2+} of 20/15 (4/3) in the absence of H_2, the following equations can be obtained for the CO oxidation at steady state

$$\frac{d\theta_{CO}}{dt} = k_1 P_{CO} \theta_{*1} - k_{-1}\theta_{CO} - k_3 \theta_{CO}\theta_O = 0$$

$$\frac{d\theta_O}{dt} = 2k_2 P_{O_2} \theta_{*2}^{2} - k_3 \theta_{CO}\theta_O = 0$$

$$\theta_{*1} + \theta_{CO} = \frac{4}{7}$$

$$\theta_{*2} + \theta_O = \frac{3}{7}$$

where θ_{CO}, θ_O, θ_{*1}, and θ_{*2} are the surface coverages of Ir−CO, O*, Ir, and Fe^{2+} sites, respectively. Based on the equation $k_i = A_i \exp(-E_i/RT)$, where A_i and E_i are adjustable parameters, the coverages θ_{CO}, θ_O, θ_{*1}, and θ_{*2} can be calculated according to the above equations once A_i and E_i are given. The reaction rates (R_{sim}) can then be calculated accordingly and compared with the experimental rates (R_{exp}) at different conditions.

The rate of formation of CO_2 can be written as $R_{sim} = k_3\theta_{CO}\theta_O$, and the parameters used in simulations are given in Table 2.

In the presence of H_2 (i.e., the PROX reaction), steps 4−7 are also involved in addition to steps 1−3. Step 4 represents the dissociative adsorption of H_2. Given that the initial heat for H_2 adsorption on the Ir−Fe/SiO_2 catalyst is low (25 kJ/mol), this step can be considered reversible at the reaction temperatures. Previous microkinetic models dealing with the PROX reaction on Pt catalysts considered the coupling between H_2 and CO that produces carboxylate or formate surface species.[28−31] To verify whether similar reaction pathways are involved in the PROX reaction over the Ir−Fe dual-site catalyst, we performed in situ DRIFTS measurements at 373 K under both H_2-free and H_2-rich atmospheres for the Ir−Fe/SiO_2 catalyst.

Table 2. Pre-Exponential Factors and Activation Energies Used in Simulations of the PROX Reaction on the Ir−Fe Catalyst

parameter	value used in simulation[a]
A_1	200
E_1	0
A_{-1}	10^{13}
E_{-1}	70
A_2	2000
E_2	0
A_3	1.3×10^6
E_3	52
A_4	1.2×10^4
E_4	0
A_{-4}	10^9
E_{-4}	39[b] (24[c])
A_5	4×10^{12}
E_5	80
A_{-5}	10^{10}
E_{-5}	60
A_6	2×10^5
E_6	40
A_7	7×10^5
E_7	40[b] (43[c])

[a] Units: s^{-1} for pre-exponential factors for surface reaction and desorption, s^{-1} Pa^{-1} for pre-exponential factors for adsorption, and kJ/mol for activation energies. [b] Parameters for the PROX reaction with H_2 concentrations of >10%. [c] Parameters for the PROX reaction with a H_2 concentration of 2%.

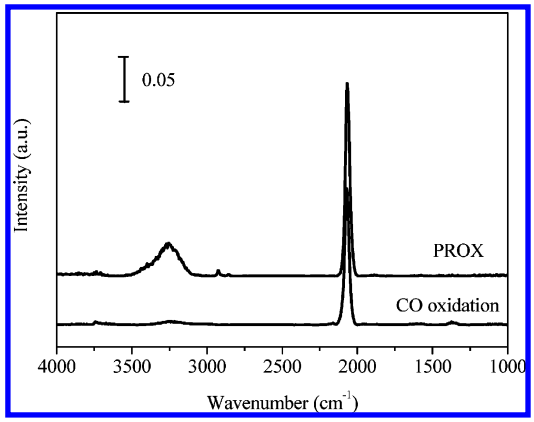

Figure 1. DRIFT spectra recorded during the PROX (40% H_2) reaction and CO oxidation at 373 K on the Ir−Fe catalyst.

As shown in Figure 1, the band positioned at 2069 cm^{-1} can be assigned to the linear adsorption of CO on Ir. In the H_2-free atmosphere, the surface carbonate or formate species can be observed in the 1000−1800 cm^{-1} range. However, these bands were almost absent in the H_2-rich atmosphere, indicating that the presence of H_2 inhibits the accumulation of carbonate or formate on the surface of Ir−Fe/SiO_2.[7−11] Therefore, the formation of surface carbonate or formate is not included in the mechanism in this study. In addition, a broad absorption band in the 3000−3500 cm^{-1} range, which can be assigned to surface OH groups or adsorbed water, was clearly observed, and the band intensity was much stronger in the PROX atmosphere as compared with that in the CO oxidation atmosphere. This result indicates that significantly more OH groups are present on the catalyst surface during the PROX reaction.

According to the DRIFTS results, the oxidation of adsorbed H and CO by adsorbed O must be included in the PROX mechanism. Because OH groups are formed by the reaction of adsorbed O and H whereas O atoms are mainly adsorbed on iron sites, it is reasonable to assume that OH groups are mainly present on the iron sites.[40] This reaction can be described in step 5. According to UBI-QEP theory, step 5 is endothermic by 23 kJ/mol, and the activation energy can be estimated to be about 88 kJ/mol for the formation of OH. Step 6 is the formation of H_2O from surface OH and H. It was reported that surface D and DO species recombined on Fe/FeO(111) to gaseous D_2O at 370 K,[41] leaving Fe on the surface. In addition, the adsorption of water on FeO was weak and led to the formation of surface hydroxyl groups, namely, FeO + H_2O = HOFeOH,[42] overcoming a high barrier. Because water was weakly bonded on the Fe species, the adsorbed water on iron sites (H_2O*) is not included in this mechanism; instead, H and OH groups form water in the gas phase directly, as shown by step 6. Step 6 is highly exothermal by 84 kJ/mol according to the UBI-QEP theory, and the activation energy is high for the dissociation of water,[42] estimated to be about 120 kJ/mol in this study. Thus, it is assumed that step 6 is irreversible. In fact, the adsorption of water on Ir−Fe sites for the formation of adsorbed H on Ir sites is highly unlikely. A similar value was reported for the dissociation of water on Fe(111).[35] Step 7 describes the surface reaction between OH adsorbed on Fe^{2+} sites and CO adsorbed on nearby Ir sites at the interface of Ir/FeO_x. It was reported that the reaction of surface CO and OH led to the formation of surface carboxyl groups[2,13] that rapidly decomposed into CO_2 and adsorbed H. Similarly, Gokhale et al.[43] studied the mechanism for the water−gas shift reaction on Cu(111) and proposed that carboxyl (COOH) groups were very reactive and difficult to identify spectroscopically because of the extremely low coverage. Accordingly, the formation of surface carboxyl groups is not included in this mechanism. Instead, a step involving the reaction of surface CO and OH to give CO_2 and surface H is included in the mechanism, as described in step 7. Because CO_2 cannot be adsorbed on the Ir−Fe/SiO_2 catalyst, step 7 is assumed to be irreversible.

Based on the ratio of active sites of Ir to Fe^{2+} in the presence of different concentration of H_2, the following equations can be obtained for the PROX reaction under steady state

$$\frac{d\theta_{CO}}{dt} = k_1 P_{CO}\theta_{*1} - k_{-1}\theta_{CO} - k_3\theta_{CO}\theta_O - k_7\theta_{CO}\theta_{OH} = 0$$

$$\frac{d\theta_O}{dt} = 2k_2 P_{O_2}\theta_{*2}^2 - k_3\theta_{CO}\theta_O - k_5\theta_H\theta_O + k_{-5}\theta_{OH}\theta_{*1} = 0$$

$$\frac{d\theta_{OH}}{dt} = k_5\theta_H\theta_O - k_{-5}\theta_{OH}\theta_{*1} - k_6\theta_H\theta_O - k_7\theta_{CO}\theta_{OH} = 0$$

$$\frac{d\theta_H}{dt} = 2k_4 P_{H_2}\theta_{*1}^2 - 2k_{-4}\theta_H^2 - k_5\theta_H\theta_O + k_{-5}\theta_{OH}\theta_{*1} - k_6\theta_H\theta_O + k_7\theta_{CO}\theta_{OH} = 0$$

$$\theta_{*1} + \theta_{CO} + \theta_H = a$$

$$\theta_{*2} + \theta_O + \theta_{OH} = 1 - a$$

*w*here θ_{CO}, θ_O, θ_H, θ_{OH}, θ_{*1}, and θ_{*2} are the surface coverages of Ir−CO, O*, Ir−H, OH*, exposed Ir, and reduced iron sites, respectively, and *a* equals 20/75, 20/88, and 20/92 corresponding to 2%, 10%, and 40% H_2 in the feed stream, respectively. The parameters used in the simulation are summarized in Table 2. The kinetic parameters for steps 1−3 were modeled for CO oxidation and adopted directly for the PROX reaction. The rates for the oxidation of CO and H_2 can be written as $R_{sim} = k_3\theta_{CO}\theta_O + k_7\theta_{CO}\theta_{OH}$ and $R_{sim} = k_6\theta_H\theta_{OH}$, respectively, which were calculated and compared to the experimental data.

4.2. Simulation Results and Discussion. Figure 2 shows the simulation results compared with the experimental data for the rate of formation of CO_2 on the Ir−Fe/SiO_2 catalyst with and without the presence of H_2 at different reaction temperatures. It is seen that the experimental data are well fitted by the

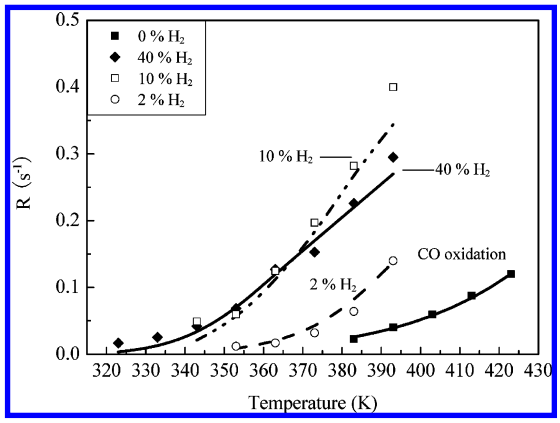

Figure 2. Simulated (lines) and experimental (points) rates in TOF versus reaction temperature for CO oxidation only and for the PROX reaction with different concentrations of H_2 in the feed stream on the Ir−Fe catalyst.

simulation curve. Because the coadsorption of CO leads to weakening of H_2 adsorption,[28,44] the adsorption heat of H_2 in the presence of 2% H_2 during the PROX reaction should be lower than that under H_2-rich (>10% H_2) conditions, and further, the activation energy of step 7 was also affected, as shown in Table 2. Accordingly, the rate constants of different steps during PROX and CO oxidation can be calculated and are listed in Table 3. For CO oxidation only (i.e., in the absence of H_2), it can be seen that the rate constant of step 3 (k_3) is 3−6 orders of magnitude smaller than those of the other two steps, indicating that the surface reaction between adsorbed CO and O is the slowest and, therefore, the rate-limiting step. On the other hand, for the PROX reaction in the presence of different concentrations of H_2 in the reaction stream, there are two steps directly involved in the formation of CO_2, steps 3 and 7. However, the rate constant of step 7 is 1−2 orders of magnitude larger than that of step 3, especially at low temperatures. According to the calculated reaction rates in Table 3, step 7 is 1−2 orders of magnitude faster than step 3. Thus, under the PROX conditions, the oxidation of CO to CO_2 is mainly through the surface reaction between adsorbed CO on Ir sites and adsorbed OH groups on Fe sites. Comparing the rate constants of steps 4, 5, and 7, one can see that step 5 (i.e., the surface reaction between O* and H* for the formation of OH) is the slowest step and, therefore, the rate-limiting step at the reaction temperatures used.

Figure 3 illustrates the effects of the partial pressure of CO on the reaction rate of CO oxidation with or without the presence of H_2. The experimental data are well fitted with the simulation lines. In the absence of H_2 (CO oxidation only), the reaction rate is zeroth-order for CO. In the presence of 40% H_2 (PROX), however, positive orders (0.37) were found for CO, which might be due to the competitive adsorption of CO and H on Ir sites. It is interesting to note that the rate for CO oxidation exhibits a negative dependence on the partial pressure of CO when 2% H_2 is present in the reaction stream. Because the H_2 concentration also affects the formation of OH on the catalyst surface whereas the OH coverage is negatively influenced by the partial pressure of CO, the rate of CO oxidation exhibits a negative-order dependence with respect to CO pressure in the presence of low concentration of H_2. On the other hand, the reaction rate, either for CO oxidation or for the PROX reaction, is independent of the partial pressure of O_2.

According to the kinetic parameters in Table 2, the coverages of different surface species can be calculated, and the results are shown in Figure 4. In the absence of H_2 (i.e., CO oxidation only), the coverages of θ_{Ir-CO} and θ_{Fe-O} are 57% and 43%, respectively, and they remain at constant values throughout the whole range of reaction temperatures concerned. As discussed above, when H_2 is absent from the reaction stream, the percentages of sites of Ir and Fe^{2+} are 57% (20/35) and 43% (15/35), respectively, for the oxidation of CO on Ir−Fe/SiO_2. Thus, all of the Ir sites are covered by CO, whereas all of the Fe^{2+} sites are covered by O during the CO oxidation only on the Ir−Fe/SiO_2 catalyst, which is consistent with results reported elsewhere.[1] On the other hand, when excess H_2 is present in the reaction stream, the coverage of each species varies with the H_2 concentration. In the presence of 2% H_2, θ_{CO} decreases slightly, whereas θ_H increases slowly with the reaction temperature. Moreover, θ_{CO} approaches its maximum value of 28% and θ_H is close to zero. This result indicates that the Ir sites are almost covered by CO even in the presence of 2% H_2 in the reaction stream. Because of the low coverage of H, the coverage of OH on the Fe^{2+} sites is also low and does not exceed the coverage of O below 393 K. In contrast, when 40% H_2 is present in the reaction stream, the coverages of CO and H on Ir sites at 323 K are calculated to be 21% and 1%, respectively, whereas they gradually approach each other (about 11%) with increasing reaction temperature. Therefore, the competition of CO and H for Ir sites becomes more pronounced at high temperatures and high concentrations of H_2, which results in a decrease of the selectivity to CO_2 formation.[7,11] On the other hand, the adsorbed O decreases and the surface OH groups increase with increasing reaction temperature, similarly to the trend for the case of 2% H_2. However, the two curves intersect at 353 K, at least 40 K lower than that in the case of 2% H_2. This result indicates that the reaction between adsorbed O and H for the formation of OH is greatly accelerated by the presence of a large excess amount of H_2 in the reaction stream. As discussed above, the percentages of sites of Ir and Fe^{2+} are 22% (20/90) and 78% (70/90), respectively, for the PROX reaction on Ir−Fe/SiO_2. At low reaction temperatures, the coverages of O and OH on iron sites are predicted to be 73% and 5%, respectively, whereas they are 4% and 74%, respectively, at high reaction temperatures. Thus, the iron sites are all covered by adsorbed O and OH groups.

Figure 5 shows the dependence of surface coverage on P_{CO} under PROX conditions. It should be pointed out that, in the case of CO oxidation only (i.e., absence of H_2 in the reaction stream), all of the Ir sites are covered by CO and all of the Fe^{2+} sites are covered by O throughout the whole temperature range from 393 to 413 K. However, in the case of PROX, it can be seen that the adsorbed OH groups on iron sites (θ_{OH}) decrease whereas the surface O on iron sites (θ_O) increases with the partial pressure of CO. At the same time, the coverage of adsorbed CO on Ir sites increases whereas the surface H decreases with increasing P_{CO} because of the competitive adsorption between CO and H_2. In the presence of 2% H_2, θ_{OH} changes more remarkably with P_{CO} than does θ_{CO}; as a result, the CO oxidation rate decreases in the PROX reaction with 2% H_2. On the contrary, θ_{CO} increases dramatically with P_{CO} with 40% H_2 in the stream, resulting in an increasing rate even though θ_{OH} keeps decreasing.

In contrast to the dependence on the partial pressure of CO, the coverages of various surface species are not affected by the partial pressure of O_2 either for CO oxidation or PROX.

Figure 6 shows the effect of the partial pressure of H_2 on the reaction rate of CO oxidation. The simulation curve fits the experimental data well. The rate of CO oxidation increases with partial pressure of H_2 until 10% of H_2 in stream and then levels off at higher H_2 partial pressures. The promotional effect of H_2 can be partially attributed to the increase of Fe^{2+} sites in the

Table 3. Calculated Reaction Rate Constants for Elementary Steps and Reaction Rates of Steps 3 and 7 for the PROX Reaction (40% H_2) on the Ir−Fe Catalyst

	T (K)						
	333	353	373	383	393	403	423
				CO Oxidation			
k_1P_{CO}/k_{-1}				141.86	81.06	40.53	28.37
$k_2P_{O_2}$				2.03×10^6	2.03×10^6	2.03×10^6	2.03×10^6
k_3 (s^{-1})				0.11	0.16	0.24	0.34
				PROX Reaction			
k_1P_{CO}/k_{-1}	3870.62	932.19	263.45	141.86	81.06		
$k_2P_{O_2}$	2.03×10^6	2.03×10^6	2.03×10^6	2.03×10^6	2.03×10^6		
k_3 (s^{-1})	0.01	0.03	0.07	0.11	0.16		
$k_4P_{H_2}/k_{-4}$	6.36×10^5	2.90×10^5	1.41×10^5	1.01×10^5	7.42×10^4		
k_5/k_{-5}	0.29	0.44	0.63	0.75	0.88		
k_6 (s^{-1})	0.11	0.24	0.50	0.70	0.97		
k_7 (s^{-1})	0.37	0.84	1.75	2.45	3.38		
r_3 (s^{-1})	0.0012	0.0018	0.0013	0.0009	0.0007		
r_7 (s^{-1})	0.0098	0.0667	0.1744	0.2254	0.2667		

Ir−Fe catalyst, as indicated in our previous report.[12] On the other hand, the partial pressure of H_2 strongly affects the coverages of surface species. As shown in Figure 7, with an increase in P_{H_2}, the surface H concentration increases, whereas the adsorbed CO amount decreases on Ir sites; concomitantly, the adsorbed O decreases, whereas the surface OH groups increase on iron sites. In particular, θ_{OH} increases quite rapidly with the partial pressure of H_2 until it reaches 10% on stream. Afterward, it increases slowly. Specifically, θ_{OH} is about 8 times more on Ir−Fe/SiO_2 at 10% H_2 than that at 2% H_2. The rapid increase in the coverage of OH on iron sites with increasing concentration of H_2 up to 10% coincides with the increase of the reaction rate of CO oxidation. Accordingly, it is suggested that OH groups on the iron sites play an important role in the PROX reaction. The increase in the coverage of OH with increasing partial pressure of H_2 can be attributed to the increase of H coverage on the surface.

The promoting effect of H_2 on the oxidation of CO through the formation of surface OH groups has also been reported by

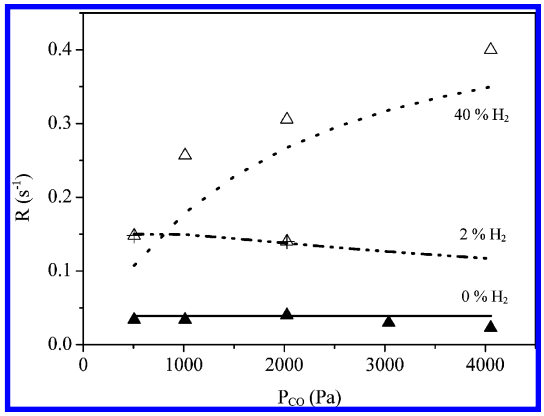

Figure 3. Simulated (lines) and experimental (points) rates in TOF versus partial pressure of CO for CO oxidation (solid line) and for the PROX reaction (40% H_2, dotted line; 2% H_2, dashed line) at 393 K on the Ir−Fe catalyst.

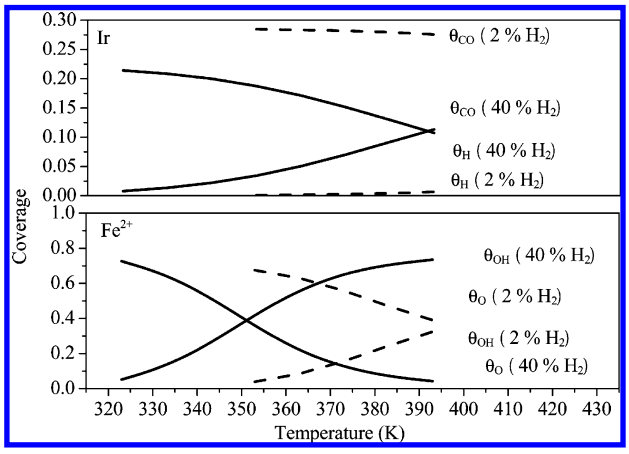

Figure 4. Coverages of different surface species versus reaction temperature for the PROX reaction with 2% and 40% H_2 in the stream on the Ir−Fe catalyst.

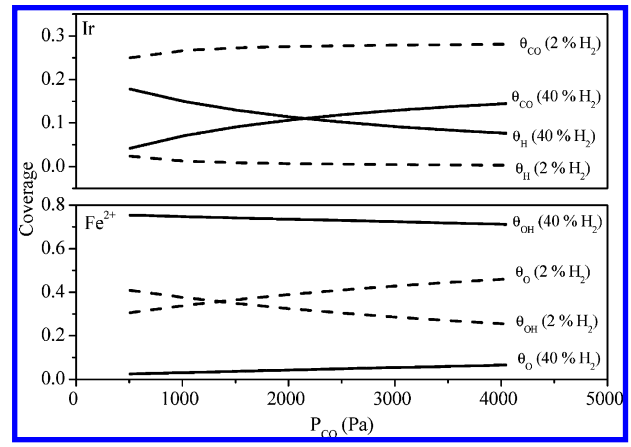

Figure 5. Coverages of different surface species versus partial pressure of CO for the PROX (40% H_2, solid line; 2% H_2, dashed line) at 393 K on the Ir−Fe catalyst.

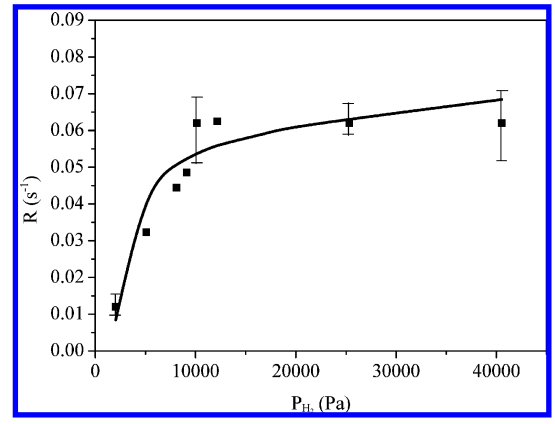

Figure 6. Simulated (lines) and experimental (points) rates in TOF versus partial pressure of H_2 for the PROX reaction at 353 K on the Ir−Fe catalyst (P_{CO} = 2026.5 Pa and P_{O_2} = 1013.25 Pa).

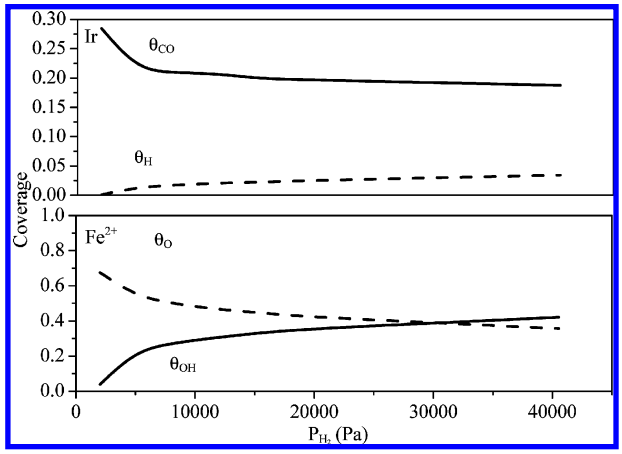

Figure 7. Coverages of different surface species versus partial pressure of H_2 for the PROX reaction at 353 K on the Ir−Fe catalyst (P_{CO} = 2026.5 Pa and P_{O_2} = 1013.25 Pa).

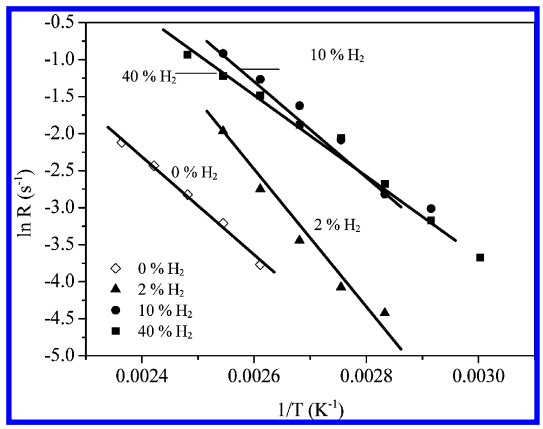

Figure 8. Simulated (lines) and experimental (points) apparent activation energies for CO oxidation with various H_2 fractions in the reaction feed on the Ir−Fe catalyst.

other researchers. Pozdnyakove-Tellinger et al.[2] observed a positive correlation between the concentration of surface OH formed by H_2 spillover from Pt and the rate of oxidation of CO, by in situ infrared spectroscopy. Mhadeshwar and Vlachos[31] pointed out that the surface OH groups were necessary in the PROX and in the water−gas shift reaction mechanism. Grabow et al.[29] studied water−gas shift reaction by density functional theory (DFT) calculations and suggested that the reaction path could be limited by the low concentration of surface OH. Tanaka et al.[45] suggested that the coadsorbed species originating from H_2 and O_2 (e.g., the OH species) under the PROX condition can promote the CO oxidation. Xu et al.[46] provided direct evidence for the interfacial $CO_{ads} + OH_{ads}$ reaction to produce CO_2 at the platinum−oxide interface at low temperatures. Our current results agree well with those reported in the literature.

The kinetic parameters modeled by the microkinetic analysis should be able to reproduce the global kinetics of the reactions.[27] Figure 8 shows the activation energies modeled for the oxidation of CO at various H_2 concentrations, compared with the data obtained experimentally. It is seen that the simulation results fit experimental data fairly well. The activation energies calculated and measured experimentally are compared in Table 4. The model predicts that the apparent activation energy for the PROX reaction decreases with increasing H_2 concentration. Because the model indicates the highest activation energy for step 5 (H* + O* ⇄ HO* + *), it is the slowest step in the PROX reaction. θ_{OH} is high at high concentrations of H_2 (>10%), and thus the oxidation of CO is mainly through the surface

Table 4. Simulation and Experimental Apparent Activation Energies for CO Oxidation with Various H_2 Fractions in the Reaction Feed on the Ir−Fe Catalyst

$y_{H_2,in}$ (%)	E_{simu} (kJ/mol)	E_{exp} (kJ/mol)	r_3 (s^{-1})	r_7 (s^{-1})
0	52	50 ± 5	0.0064	−
2	77	72 ± 10	0.0051	0.0034
10	54	45 ± 5	0.0026	0.0503
40	48	44 ± 5	0.0018	0.0667

reaction between adsorbed CO and surface OH groups. On the other hand, θ_{OH} is low at low concentrations of H_2 (e.g., 2%), and the oxidation of CO might be through two pathways, namely, steps 3 and 7. This might be the case for the PROX reaction on Ir−Fe/SiO_2 when 2% H_2 is present. The model predicts that 40% of the CO is oxidized through step 7 whereas the other 60% of CO is oxidized through step 3. On the other hand, the model predicts that step 3 is extremely slow and that almost 100% of CO is oxidized through step 7 on the Ir−Fe/SiO_2 when 10% and 40% of H_2 are present for the PROX reaction. Thus, the activation energy and reaction rate are affected by the coverages of different surface species.[28,29] Surprisingly, in the absence of H_2, both the activation energy and rate of oxidation of CO are low, as compared to the case of PROX at 2% H_2. Quinet et al.[8] observed the similar phenomenon on a gold catalyst. This can also be explained by the model. Without the presence of H_2, the oxidation of CO could only proceed through step 3, which is a slow step with a low activation energy. At low concentration of H_2 (2%), the presence of an additional pathway, namely, the reaction of adsorbed CO with surface OH (step 7) increases the rate for the oxidation of CO. However, the formation of OH (step 5) is a step with a high activation energy, which might be the limiting step for the PROX reaction at low concentration of H_2 (2%). When the concentration of H_2 increases to 10% or 40%, a great amount of surface OH groups are formed, step 5 is then no longer the limiting step, and step 7 becomes rate-limiting. That might be the reason why the overall activation energy decreases again when the concentration of H_2 increases above 10%.

Because the model predicts the important roles of surface OH groups in the PROX reaction, further work should be directed toward increasing the concentration of surface OH groups. Experimentally, this can be achieved by adding water to the reaction stream and using a ferric hydroxide to support Ir. Further studies are currently being conducted in our group.

5. Conclusions

We have presented herein a detailed microkinetic study of CO oxidation and the PROX reaction on bimetallic Ir−Fe catalyst. The elementary steps, coverages of different intermediates, activation energies, and reaction mechanism for the PROX reaction and CO oxidation were obtained through a combination of microkinetic modeling and experimental studies. The experimental data, which covered a wide range of temperature and gas feed compositions, were well fitted by the simulated data calculated from our microkinetic model, which confirms the validity of our model.

For CO oxidation, no competitive adsorption between CO and O_2 was observed. Both the adsorption of CO and O_2 reached saturation on Ir and Fe^{2+}, respectively, and the coverages of CO and O were irrelevant to the partial pressure of CO or O_2. The surface reaction between CO and O was the slowest step and, therefore, the rate-determining step.

For the PROX reaction, CO can be oxidized not only by atomic O, but also by the surface OH formed by reaction of

atomic O and H. The coverages of H and OH increase whereas the coverage of O decreases with increasing reaction temperature. The CO oxidation rate is insensitive to the pressure of O_2, yet it increases with increasing partial pressure of either CO or H_2 for the PROX reaction under H_2-rich conditions.

The model suggests that the dominant PROX reaction path goes through CO oxidation by surface OH, rather than by atomic O. The formation of OH was the slowest step and, therefore, the rate-determining step, which is different from the mechanism of CO oxidation. The variation in the apparent activation energy with different H_2 concentrations is due to the change in the coverage of surface species, especially the coverage of OH. In addition to maintaining enough Fe^{2+} sites for oxygen activation, H_2 also directly participates in the reaction by forming OH groups.

Acknowledgment

Financial support from the Chinese Academy of Sciences for the "100 Talents" project and the National Science Foundation of China (20325620, 20773122, 20773124, 21003119, and 20673055) is thankfully acknowledged.

Literature Cited

(1) Sirijaruphan, A.; Goodwin, J. G., Jr.; Rice, R. W. Effect of Fe promotion on the surface reaction parameters of Pt/γ-Al_2O_3 for the selective oxidation of CO. *J. Catal.* **2004**, *224*, 304.

(2) Pozdnyakove-Tellinger, O.; Teschner, D.; Kröhnert, J.; Jentoft, F. C.; Knop-Gericke, A.; Schlögl, R.; Wootsch, A. Surface water-assisted preferential CO oxidation on Pt/CeO_2 catalyst. *J. Phys. Chem. C* **2007**, *111*, 5426.

(3) Boccuzzi, F.; Chiorino, A. FTIR study of CO oxidation on Au/TiO_2 at 90 K and room temperature. An insight into the nature of the reaction centers. *J. Phys. Chem. B* **2000**, *104*, 5414.

(4) Huang, Y. Q.; Wang, A. Q.; Li, L.; Wang, X. D.; Su, D. S.; Zhang, T. "Ir-in-ceria": A highly selective catalyst for preferential CO oxidation. *J. Catal.* **2008**, *225*, 144.

(5) Schubert, M. M.; Hackenberg, S.; van Veen, A. C.; Muhler, M.; Plzak, V.; Behm, R. J. CO oxidation over supported gold catalysts—"Inert" and "active" support materials and their role for the oxygen supply during reaction. *J. Catal.* **2001**, *197*, 113.

(6) Kotobuki, M.; Watanabe, A.; Uchida, H.; Yamashita, H.; Watanabe, M. Reaction mechanism of preferential oxidation of carbon monoxide on Pt, Fe, and Pt−Fe/mordenite catalysts. *J. Catal.* **2005**, *236*, 262.

(7) Denkwitz, Y.; Schumacher, B.; Kuèerová, G.; Behm, R. J. Activity, stability, and deactivation behavior of supported Au/TiO_2 catalysts in the CO oxidation and preferential CO oxidation reaction at elevated temperatures. *J. Catal.* **2009**, *267*, 78.

(8) Quinet, E.; Morfin, F.; Diehl, F.; Avenier, P.; Caps, V.; Rousset, J.-L. Hydrogen effect on the preferential oxidation of carbon monoxide over alumina-supported gold nanoparticles. *Appl. Catal. B* **2008**, *80*, 195.

(9) Tanaka, K.; Shou, M.; He, H.; Shi, X. Y.; Zhang, X. L. Dynamic characterization of the intermediates for low-temperature PROX reaction of CO in H_2—Oxidation of CO with OH via HCOO intermediate. *J. Phys. Chem. C* **2009**, *113*, 12427.

(10) Schumacher, B.; Denkwitz, Y.; Plzak, V.; Kinne, M.; Behm, R. J. Kinetics, mechanism, and the influence of H_2 on the CO oxidation reaction on a Au/TiO_2 catalyst. *J. Catal.* **2004**, *224*, 449.

(11) Zhang, W. S.; Huang, Y. Q.; Wang, J.; Liu, K.; Wang, X. D.; Wang, A. Q.; Zhang, T. $IrFeO_x/SiO_2$—A highly active catalyst for preferential CO oxidation in H_2. *Int. J. Hydrogen Energy* **2010**, *35*, 3065.

(12) Liu, K.; Wang, A. Q.; Zhang, W. S.; Wang, J.; Huang, Y. Q.; Wang, X. D.; Shen, J. Y.; Zhang, T. Quasi in situ ^{57}Fe Mössbauer spectroscopic study: Quantitative correlation between Fe^{2+} and H_2 concentration for PROX over Ir−Fe/SiO_2 catalyst. *J. Phys. Chem. C* **2010**, *114*, 8533.

(13) Bergeld, J.; Kasemo, B.; Chakarov, D. V. CO oxidation on Pt(111) promoted by coadsorbed H_2O. *Surf. Sci.* **2001**, *495*, L 815.

(14) Kahlich, M. J.; Gasteiger, H. A.; Behm, R. J. Kinetics of the selective CO oxidation in H_2-rich gas on Pt/Al_2O_3. *J. Catal.* **1997**, *171*, 93.

(15) Sirijaruphan, A.; Goodwin, J. G., Jr.; Rice, R. W. Effect of temperature and pressure on the surface kinetic parameters of Pt/γ-Al_2O_3 during selective CO oxidation. *J. Catal.* **2004**, *227*, 547.

(16) Kim, D. H.; Lim, M. S. Kinetics of selective CO oxidation in hydrogen-rich mixtures on Pt/alumina catalysts. *Appl. Catal. A* **2002**, *224*, 27.

(17) Amphlett, J. C.; Mann, R. F.; Peppley, B. A. On board hydrogen purification for steam reformation/PEM fuel cell vehicle power plants. *Int. J. Hydrogen Energy* **1996**, *21*, 673.

(18) Han, Y.-F.; Kahlich, M. J.; Kinne, M.; Behm, R. J. Kinetic study of selective CO oxidation in H_2-rich gas on a Ru/γ-Al_2O_3 catalyst. *Phys. Chem. Chem. Phys.* **2002**, *4*, 389.

(19) Choi, Y.; Stenger, H. G. Kinetics, simulation and insights for CO selective oxidation in fuel cell applications. *J. Power Sources* **2004**, *129*, 246.

(20) Schubert, M. M.; Kahlich, M. J.; Feldmeyer, G.; Hüttner, M.; Hackenberg, S.; Gasteiger, H. A.; Behm, R. J. Bimetallic PtSn catalyst for selective CO oxidation in H_2-rich gases at low temperatures. *Phys. Chem. Chem. Phys.* **2001**, *3*, 1123.

(21) Lynggaard, H.; Andreasen, A.; Stegelmann, C.; Stoltze, P. Analysis of simple kinetic models in heterogeneous catalysis. *Prog. Surf. Sci.* **2004**, *77*, 71.

(22) Broadbelt, L. J.; Snurr, R. Q. Applications of molecular modeling in heterogeneous catalysis research. *Appl. Catal. A* **2000**, *200*, 23.

(23) Stoltze, P. Microkinetic simulation of catalytic reactions. *Prog. Surf. Sci.* **2000**, *65*, 65.

(24) Cortright, R. D.; Dumesic, J. A. Kinetics of heterogeneous catalytic reactions: Analysis of reaction schemes. *Adv. Catal.* **2001**, *46*, 161.

(25) Campbell, C. T. Micro- and macro-kinetics: Their relationship in heterogeneous catalysis. *Top. Catal.* **1994**, *1*, 353.

(26) Oh, S. H.; Fischer, G. B.; Carpenter, J. E.; Goodman, D. W. Comparative kinetic studies of CO---O_2 and CO---NO reactions over single crystal and supported rhodium catalysts. *J. Catal.* **1986**, *100*, 360.

(27) Dumesic, J. A.; Rudd, D. A.; Aparicio, L. M.; Rekoske, J. E.; Treviño, A. A. *The Microkinetics of Heterogeneous Catalysis*; American Chemical Society: Washington, DC, 1993.

(28) Mhadeshwar, A. B.; Vlachos, D. G. Hierarchical, multiscale surface reaction mechanism development: CO and H_2 oxidation, water−gas shift, and preferential oxidation of CO on Rh. *J. Catal.* **2005**, *234*, 48.

(29) Grabow, L. C.; Gokhale, A. A.; Evans, S. T.; Dumesic, J. A.; Mavrikakis, M. Mechanism of the water gas shift reaction on Pt: First principles, experiments, and microkinetic modeling. *J. Phys. Chem. C* **2008**, *112*, 4608.

(30) Park, Y. K.; Aghalayam, P.; Vlachos, D. G. A generalized approach for predicting coverage-dependent reaction parameters of complex surface reactions: Application to H_2 oxidation over platinum. *J. Phys. Chem. A* **1999**, *103*, 8101.

(31) Mhadeshwar, A. B.; Vlachos, D. G. Microkinetic modeling for water-promoted CO oxidation, water−gas shift, and preferential oxidation of CO on Pt. *J. Phys. Chem. B* **2004**, *108*, 15246.

(32) Raimondeau, S.; Aghalayam, P.; Mhadeshwar, A. B.; Vlachos, D. G. Parameter optimization of molecular models: Application to surface kinetics. *Ind. Eng. Chem. Res.* **2003**, *42*, 1174.

(33) Ovesen, C. V.; Clausen, B. S.; Hammershøi, B. S.; Steffensen, G.; Askgaard, T.; Chorkendorff, I.; Nørskov, J. K.; Rasmussen, P. B.; Stoltze, P.; Taylor, P. A microkinetic analysis of the water−gas shift reaction under industrial conditions. *J. Catal.* **1996**, *158*, 170.

(34) Shustorovich, E.; Sellers, H. The UBI-QEP method: A practical theoretical approach to understanding chemistry on transition metal surfaces. *Surf. Sci. Rep.* **1998**, *31*, 1.

(35) Hei, M. J.; Chen, H. B.; Yi, J.; Lin, Y. J.; Lin, Y. Z.; Wei, G.; Liao, D. W. CO_2-reforming of methane on transition metal surfaces. *Surf. Sci.* **1998**, *417*, 82.

(36) Zhang, W. S.; Wang, A. Q.; Li, L.; Wang, X. D.; Zhang, T. Design of a novel bifunctional catalyst IrFe/Al_2O_3 for preferential CO oxidation. *Catal. Today* **2008**, *131*, 457.

(37) Sun, Y.-N.; Qin, Z.-H.; Lewandowski, M.; Carrasco, E.; Sterrer, M.; Shaikhutdinov, S.; Freund, H.-J. Monolayer iron oxide film on platinum promotes low temperature CO oxidation. *J. Catal.* **2009**, *266*, 359.

(38) Azzam, K. G.; Babich, I. V.; Seshan, K.; Lefferts, L. Bifunctional catalysts for single-stage water−gas shift reaction in fuel cell applications. Part 1. Effect of the support on the reaction sequence. *J. Catal.* **2007**, *251*, 153.

(39) Akın, A. N.; Kılaz, G.; İşli A., İ; Önsan, Z. İ. Development and characterization of Pt−SnO_2/γ-Al_2O_3 catalysts. *Chem. Eng. Sci.* **2001**, *56*, 881.

(40) Pozdnyakova, O.; Teschner, D.; Wootsch, A.; Kröhnert, J.; Steinhauer, B.; Sauer, H.; Toth, L.; Jentoft, F. C.; Knop-Gericke, A.; Paál, Z.; Schlögl, R. Preferential CO oxidation in hydrogen (PROX) on ceria-supported catalysts. Part I: Oxidation state and surface species on Pt/CeO_2 under reaction conditions. *J. Catal.* **2006**, *237*, 1.

(41) Parkinson, G. S.; Kim, Y. K.; Dohnálek, Z.; Smith, R. S.; Kay, B. D. Reactivity of Fe^0 atoms and clusters with D_2O over FeO (111). *J. Phys. Chem. C* **2009**, *113*, 4960.

(42) Mebel, A. M.; Hwang, D.-Y. Theoretical study of the reaction mechanism of Fe atoms with H_2O, H_2S, O_2 and H^+. *J. Phys. Chem. A* **2001**, *105*, 7460.

(43) Gokhale, A. A.; Dumesic, J. A.; Mavrikakis, M. On the mechanism of low-temperature water gas shift reaction on copper. *J. Am. Chem. Soc.* **2008**, *130*, 1402.

(44) Diemant, T.; Hager, T.; Hoster, H. E.; Rauscher, H.; Behm, R. J. Hydrogen adsorption and coadsorption with CO on well-defined bimetallic PtRu surfaces—A model study on the CO tolerance of bimetallic PtRu anode catalysts in low temperature polymer electrolyte fuel cells. *Surf. Sci.* **2003**, *541*, 137.

(45) Tanaka, H.; Kuriyama, M.; Ishida, Y.; Ito, S.; Kubota, T.; Miyao, T.; Naito, S.; Tomishige, K.; Kunimori, K. Preferential CO oxidation in hydrogen-rich stream over Pt catalysts modified with alkali metals. Part II. Catalyst characterization and role of alkali metals. *Appl. Catal. A* **2008**, *343*, 125.

(46) Xu, L.; Ma, Y.; Zhang, Y.; Jiang, Z.; Huang, W. Direct evidence for the interfacial oxidation of CO with hydroxyls catalyzed by Pt/oxide nanocatalysts. *J. Am. Chem. Soc.* **2009**, *131*, 16366.

Received for review April 18, 2010
Revised manuscript received October 6, 2010
Accepted November 5, 2010

IE1009052